AMERICAN SOCIETY FOR MICROBIOLOGY | Journal of Virology®

VACCINES AND ANTIVIRAL AGENTS

A Measles Virus-Based Vaccine Candidate Mediates Protection against Zika Virus in an Allogeneic Mouse Pregnancy Model

Cindy Nürnberger,[a,b] Bianca S. Bodmer,[a] Anna H. Fiedler,[a,b] Gülsah Gabriel,[c,d] Michael D. Mühlebach[a,b]

[a]Veterinary Medicine Division, Paul-Ehrlich-Institut, Langen, Germany
[b]German Center for Infection Research, Gießen-Marburg-Langen, Germany
[c]Heinrich Pette Institute, Leibniz Institute for Experimental Virology, Hamburg, Germany
[d]Institute for Virology, University of Veterinary Medicine, Hannover, Germany

ABSTRACT The impact of the Zika virus (ZIKV) epidemic highlights the need for vaccines that reduce or prevent infection and reliably prevent teratogenic complications. The live-attenuated measles virus (MV) vaccine strains are a promising vaccine platform, since they induce robust humoral and cellular immune responses against additional antigens and have an excellent safety record. To explore its potential to protect against ZIKV, we compared a recombinant Schwarz strain MV that encodes ZIKV prM and soluble E proteins (MV-Zika-sE) with a prototypic alum-adjuvanted whole inactivated ZIKV particle vaccine. Analysis of MV-Zika-sE-infected cells confirmed antigen expression, and the virus replicated with vaccine strain characteristics. Immunized IFNAR$^{-/-}$-CD46Ge mice developed E protein-specific and neutralizing antibodies, and ZIKV E-specific cellular immune responses were observed by gamma interferon (IFN-γ) enzyme-linked immunospot (ELISpot) and *in vitro* T cell proliferation assays. To analyze protective efficacy, vaccinated female mice were challenged with ZIKV after allogeneic mating. In MV-Zika-sE-vaccinated mice, weight gain was similar to that in uninfected mice, while no plasma viremia was detectable in the majority of the animals. In contrast, infected control animals gained less weight and experienced about 100-fold higher viremia over at least 3 days. Moreover, vaccination with MV-Zika-sE reduced the ZIKV load in different organs and the placentas and prevented infection of the fetus. Consequently, no fetal growth retardation, anemia, or death due to ZIKV infection was seen in MV-Zika-sE-vaccinated dams. In contrast, the inactivated ZIKV vaccine had little to no effect in our studies. Therefore, the MV-derived ZIKV vaccine is a promising candidate for further preclinical and clinical development.

IMPORTANCE Zika virus (ZIKV) is a mosquito-borne flavivirus that causes a variety of neurological complications, including congenital birth defects. Despite the urgent need, no ZIKV vaccine has yet been licensed. Recombinant vaccine strain-derived measles viruses (MV) constitute a promising vector platform to induce immunity against foreign pathogens by expressing antigens from additional transcription units while at the same time possessing a remarkable safety profile. This concept has already been validated against different pathogens, including at least 3 other flaviviruses, and our data show that vaccination with MV expressing soluble ZIKV E protein significantly diminishes infection and prevents fetal loss or damage in an allogeneic mouse pregnancy model. It can thus be regarded as a promising emergency vaccine candidate with the potential for inclusion in routine vaccination settings in areas of endemicity to prevent teratogenic effects of circulating ZIKV during pregnancy, comparable to standard rubella virus vaccination.

KEYWORDS measles virus, ZIKV pathology, Zika virus, allogeneic pregnancy model, immunization, teratogenic infection, vaccines

Citation Nürnberger C, Bodmer BS, Fiedler AH, Gabriel G, Mühlebach MD. 2019. A measles virus-based vaccine candidate mediates protection against Zika virus in an allogeneic mouse pregnancy model. J Virol 93:e01485-18. https://doi.org/10.1128/JVI.01485-18.

Editor Mark T. Heise, University of North Carolina at Chapel Hill

Address correspondence to Michael D. Mühlebach, Michael.Muehlebach@pei.de.

C.N. and B.S.B. contributed equally to this work.

Received 27 August 2018
Accepted 27 October 2018
Accepted manuscript posted online 14 November 2018
Published 17 January 2019

Due to an ongoing epidemic in the Americas since 2015, Zika virus (ZIKV) has raised worldwide concerns by causing congenital neurological abnormalities in babies of ZIKV-infected mothers. Such fetal phenotypes have been described as congenital ZIKV syndrome (1). A total of 26,000 suspected cases of ZIKV disease in pregnant women were reported between January 2016 and June 2017 in Brazil, 11,500 of which were confirmed in the laboratory. Moreover, 3,000 out of 14,500 suspected cases of microcephaly and congenital ZIKV syndrome reported from August 2015 until July 2017 were validated by clinical, radiological, or laboratory detection methods. Thus, more than one-third of 582 fetal deaths after birth or during pregnancy and cases of microcephaly or other fetal malformations of the central nervous system reported in 2016 in Brazil were found to be associated with ZIKV infection of the mothers during pregnancy (2). Therefore, the development of effective countermeasures is regarded as essential, especially for women of reproductive age, and ZIKV has consequently been included as a priority pathogen in the list of the World Health Organization (WHO) (3). While antivirals may serve as fast emergency measures in a diagnosed infection, the development of a prophylactic vaccine that also prevents fetal ZIKV infection during pregnancy is regarded as urgent. For this purpose, the WHO has assembled a ZIKV vaccine target product profile (TPP) with desirable characteristics of an emergency ZIKV vaccine. Accordingly, development of a prophylactic ZIKV vaccine is of highest priority for the vaccination of women of childbearing age via an emergency vaccination scheme to prevent congenital sequela of ZIKV infection. This approach potentially includes pregnant women, as well (4).

ZIKV is a mosquito-borne flavivirus and is mainly transmitted by *Aedes aegypti* mosquitos, which also serve as vectors for related flaviviruses, such as Dengue virus (DENV) or yellow fever virus (YFV) (5). In addition, ZIKV has been found to be efficiently transmitted sexually, with the ability to persist in the vaginal epithelium and body fluids like semen (6). ZIKV is named after the location of its first isolation in 1947, the Zika Forest in Uganda (7). It initially drew little attention due to the historically generally mild or asymptomatic course of infection (8, 9). However, the virus was detected during an outbreak on Yap Island in Micronesia in 2007 (10) and was introduced into South America in 2014 after a stopover in French Polynesia in 2013 (11, 12). By that time, the pathology of ZIKV infections had changed quite dramatically, including the teratogenic effects that have triggered worldwide research activities and declaration of ZIKV as a global health emergency of international concern on 1 February 2016.

Inactivated whole-virus preparations, which especially induce antibody responses but lack induction of cytotoxic T cells (13, 14), are the basis for several licensed flavivirus vaccines (15, 16). As an alternative, DNA vaccines with a strong bias for induction of T cell immunity (17, 18) have been tested as a quickly generated emergency vaccine platform (19, 20). Both technologies can be considered safe because of the lack of pathogen replication. However, such vaccine concepts are often less effective than live-attenuated vaccines (LAVs), such as the highly effective YFV vaccine 17D (21), which was obtained by serial passaging of the pathogenic YFV Asibi strain (22). LAVs present the respective antigens in higher abundance; in their "physiological" localization; and in the context of a real, albeit attenuated, infection, which still releases danger- and pathogen-associated molecular patterns. Thus, LAVs usually induce higher-affinity antibodies, more robust immune memory, and a stronger $CD8^+$ cytotoxic T cell response than inactivated antigen preparations or subunit vaccines (23, 24).

Unfortunately, the development of a live-attenuated vaccine strain for a newly emerging pathogen is time-consuming and has an inherent risk of failure due to lack of proper and stable attenuation. To combine the efficacy of a LAV with the safety profile of an inactivated or subunit/DNA vaccine, well-characterized safe and efficacious vaccine strains can be genetically engineered to present critical antigens of the emerging pathogen of interest. A recent example is the Ebola vaccine, which showed efficacy in a phase III trial (25) and is based on vesicular stomatitis virus (VSV). Among others, measles virus (MV) vaccine strains have been developed as a platform technology for vaccine development (26) and have shown immunogenicity and efficacy

against flavivirus infections in animal models for DENV (27), West Nile virus (28), and Japanese encephalitis virus (29). For ZIKV, an MV-based vaccine that encodes ZIKV envelope antigens has been developed by Themis Bioscience and is currently being tested in a phase I clinical trial (NCT02996890).

In this study, we aimed to compare this recombinant live-attenuated ZIKV vaccine candidate, MV-Zika-sE, based on the MV Schwarz vaccine strain (MV_{Schw}), which additionally encodes a soluble version of ZIKV envelope protein E, to a preparation of Zika purified formalin-inactivated virus (ZPIV) mimicking standard flavivirus vaccines. To characterize this vaccine candidate, we first analyzed its replication efficiency and the expression of the additional ZIKV antigens of two different clones (#4 and #11) *in vitro*. After characterizing the humoral and cellular immune responses induced in vaccinated MV receptor-transgenic $IFNAR^{-/-}$-CD46Ge mice, we assessed the protection conferred on vaccinated animals themselves, as well as their unborn, allogeneic offspring, in an adapted allogeneic ZIKV challenge model in pregnant mice.

RESULTS

Characterization of recombinant MV encoding a soluble form of the ZIKV envelope protein. To compare a bivalent MV/ZIKV vaccine that is tested in clinical studies to a mimic of standard flaviviral vaccines, i.e., a preparation of purified inactivated ZIKV (ZPIV), two vaccine clones of so-called MV-Zika-sE were purchased after generation and sequence verification of the clones. For generation of the bivalent MV/ZIKV vaccine, a truncated version of the ZIKV E protein was designed that lacks the stem-anchor region of E and thus gives rise to a soluble E protein (sE). For proper expression and folding of the flaviviral E proteins, the pre-membrane protein (prM) is needed (30). In addition, the signal peptide (SP) at the carboxy-terminal end of the capsid protein is necessary at the amino terminus of the recombinant antigen for the desired exocytic trafficking via the secretory pathway. Therefore, a gene encoding the fusion protein of ZIKV (strain BeH818995; GenBank accession no. KU365777.1) prM-sE preceded by the respective SP-encoding sequence from the carboxy-terminal end of the capsid (C) protein was codon optimized and generated by gene synthesis (Fig. 1A). This recombinant gene was inserted into an additional transcription unit (ATU) following the MV phosphoprotein (P) gene cassette of recombinant Schwarz vaccine strain measles virus MV_{Schw}.

The respective recombinant vaccine clones were generated using this plasmid, and two vaccine clones (MV-Zika-sE#4 and MV-Zika-sE#11), here designated MV-sE#4 and MV-sE#11, respectively, were obtained and used for further characterization, together with MV_{Schw}-GFP control vaccine virus (MV-GFP) encoding the green fluorescent protein (GFP) in the same genomic position.

Expression of E protein in MV-Zika-sE-infected Vero cells was demonstrated by immunostaining (Fig. 1B) but was also detectable in the cell culture supernatant (data not shown). Possible differences in expression levels were analyzed via immunoblot analysis (Fig. 1C). While formation of syncytia indicative of MV infection was seen in all infected samples, only Vero cells infected with MV-sE#4 and MV-sE#11 revealed specific expression of ZIKV E protein in these areas (Fig. 1B), indicating homogeneity of the vaccine virus population. Expression and processing of prM have not been separately analyzed. However, the SP-prM-sE antigen can be translated only as a polyprotein and must subsequently be cleaved during transport via the secretory pathway, presumably by host signal peptidases, so that sE can be released by the infected cells, as observed. Therefore, we concluded that SP-prM must be expressed and guides sE to the secretory pathway, while at least M stays associated with infected cells' membranes because of its membrane-spanning segments even after potential furin cleavage of the pr peptide. Expression of the ZIKV antigens had no effect on replication, as shown by a multistep growth kinetic of cell-associated (Fig. 1E) and released (Fig. 1D) virus. Titers of both MV_{Schw}-sE clones and the control virus MV-GFP reached similar maximum values exceeding 1×10^5 50% tissue culture infective doses ($TCID_{50}$)/ml at 4 days postinfection (dpi) in the supernatant. Cell-associated virus titers peaked at 3 dpi at approxi-

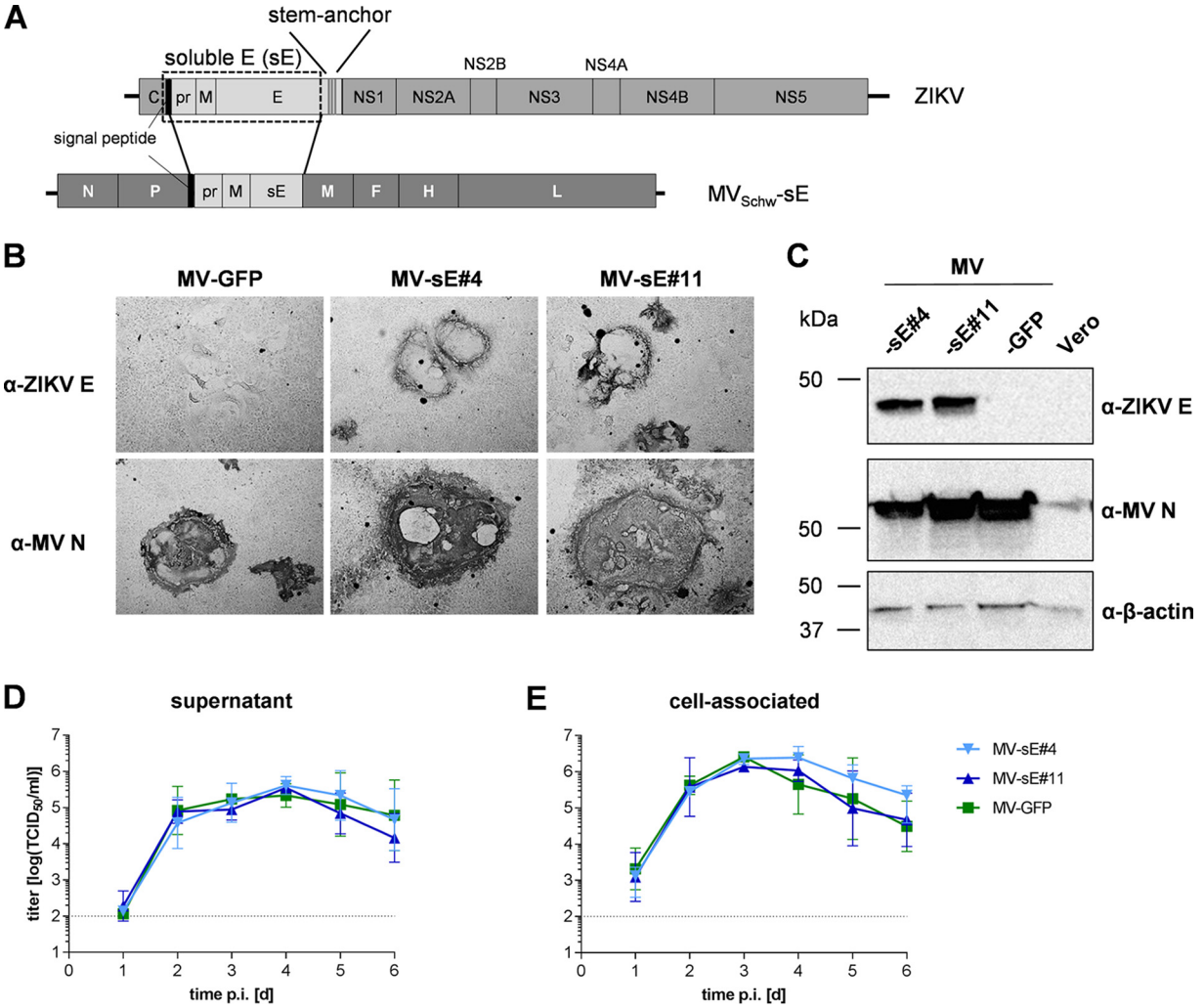

FIG 1 Characterization of recombinant MV expressing a soluble form of the ZIKV E protein. (A) A truncated version of the ZIKV E protein gene lacking the stem-anchor region, resulting in sE, was inserted together with the prM gene preceded by the C-terminal signal peptide of the capsid (C) sequence, indicated by a black bar, into an additional transcription unit following the P gene cassette of the MV_{Schw} genome. (B and C) ZIKV E protein expression in Vero cells was verified via immunoperoxidase monolayer assay (IPMA) (B) or Western blot analysis (C) directly comparing two clones of MV-Zika-sE encoding soluble E (MV-sE#4 and MV-sE#11) to control MV_{Schw} virus encoding GFP (MV-GFP). The blots and fixed cells were probed as indicated. The apparent molecular weight is also indicated. (D and E) Multistep growth kinetics of the indicated recombinant MV (P4) on Vero cells at an MOI of 0.03. Shown are titers of cell-associated virus (E), as well as virus in the cell supernatant (D), of samples at the indicated time points postinfection titrated on Vero cells. Means and standard deviations of the results of three independent experiments and the lower limit of detection (LLD) (dotted lines) of 1×10^2 $TCID_{50}$/ml are depicted.

mately 1×10^6 $TCID_{50}$/ml. In conclusion, recombinant MV_{Schw} encoding ZIKV prM-sE mediated expression of a soluble form of the E protein in all infected cells and still replicated with control virus characteristics.

Recombinant MV encoding soluble ZIKV prM-sE protein induces ZIKV E-specific humoral immune responses. To analyze humoral immunity induced by MV-Zika-sE, $IFNAR^{-/-}$-CD46 mice ($n = 4$ to 6) were vaccinated with both clones, the control MV-GFP, or medium (mock) in a prime-boost regimen at days 0 and 21, each time with 5×10^4 $TCID_{50}$. Serum samples were taken at days 0, 21, and 42 (Fig. 2A). The induction of ZIKV-specific humoral immune responses was analyzed using a ZIKV prM- or E-specific enzyme-linked immunosorbent assay (ELISA). Twenty-one days after the first immunization, MV-sE-vaccinated mice developed specific ZIKV E-binding IgG titers ranging from 160 U/ml to 2,200 U/ml, with mean titers of approximately 1,000 U/ml for both vaccine clones (Fig. 2B). Three weeks after the boost, anti-E IgG titers in the mice had increased to 5,000 U/ml, with similar mean concentrations for both clones. Serum

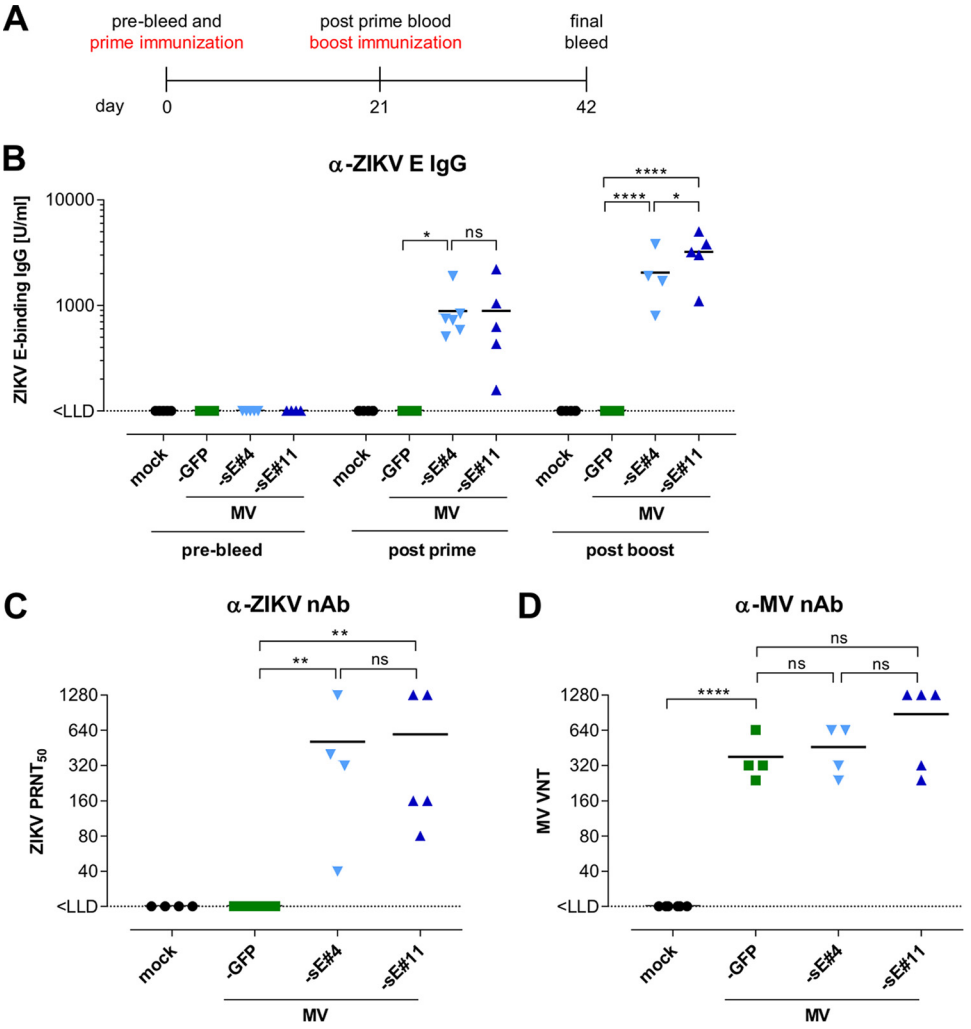

FIG 2 Humoral immunity induced by recombinant MV vaccines. (A) Schematic depiction of vaccination schedule and subsequent analysis. IFNAR$^{-/-}$-CD46Ge mice (n = 4 to 6) were immunized with 5×10^4 $TCID_{50}$ of the ZIKV vaccine clone MV-sE#4 or MV-sE#11, MV-GFP vaccine control virus, or medium (mock) on days 0 and 21. Before immunization and 21 days after boost vaccination, blood was drawn for analysis of humoral immunity. (B) ZIKV E-specific total IgG antibody titers were determined by ELISA (LLD = 100 U/ml). (C) Functional ZIKV neutralizing antibodies (nAb) were determined in the postboost sera (day 42) via plaque reduction neutralization assay of ZIKV plaques ($PRNT_{50}$) on Vero cells (LLD = 20 $PRNT_{50}$/ml). (D) VNT against MV in sera of mice after boost immunization were calculated as reciprocals of the highest dilution abolishing infectivity of 50 PFU of MV. One-way analysis of variance (ANOVA) with Tukey multiple comparison was used for statistics. ns, not significant; *, $P < 0.05$; **, $P < 0.01$; ****, $P < 0.0001$. The horizontal lines indicate mean values. MV-sE#4 and MV-sE#11 are depicted as light- and dark-blue triangles, and MV-GFP is depicted as green squares.

samples from control mice did not reveal any ZIKV E-specific IgG throughout the experiment, and no prM-specific IgG was induced in any mice (data not shown). Next, the functionality of the ZIKV-specific antibodies was assessed by a plaque reduction neutralization test (PRNT). The neutralization capacities of anti-ZIKV antibodies induced by MV-Zika-sE 21 days after boost immunization were comparable for both analyzed vaccine clones, i.e., 50% plaque reduction neutralization titers ($PRNT_{50}$) of 40 to 1,280 in mice immunized with MV-sE#4 and 80 to 1,280 in mice immunized with MV-sE#11, with mean titers of approximately 512 (Fig. 2C). In contrast, serum samples of unvaccinated or control-vaccinated mice did not neutralize ZIKV ($PRNT_{50} < 20$).

To assess coinduced anti-measles virus immunity, all sera were analyzed for neutralizing activity against MV. For this purpose, MV-specific neutralizing antibodies (virus neutralizing titers [VNT]) were quantified (Fig. 2D). After the boost immunization, all sera of mice vaccinated with MV contained similar levels of neutralizing antibodies

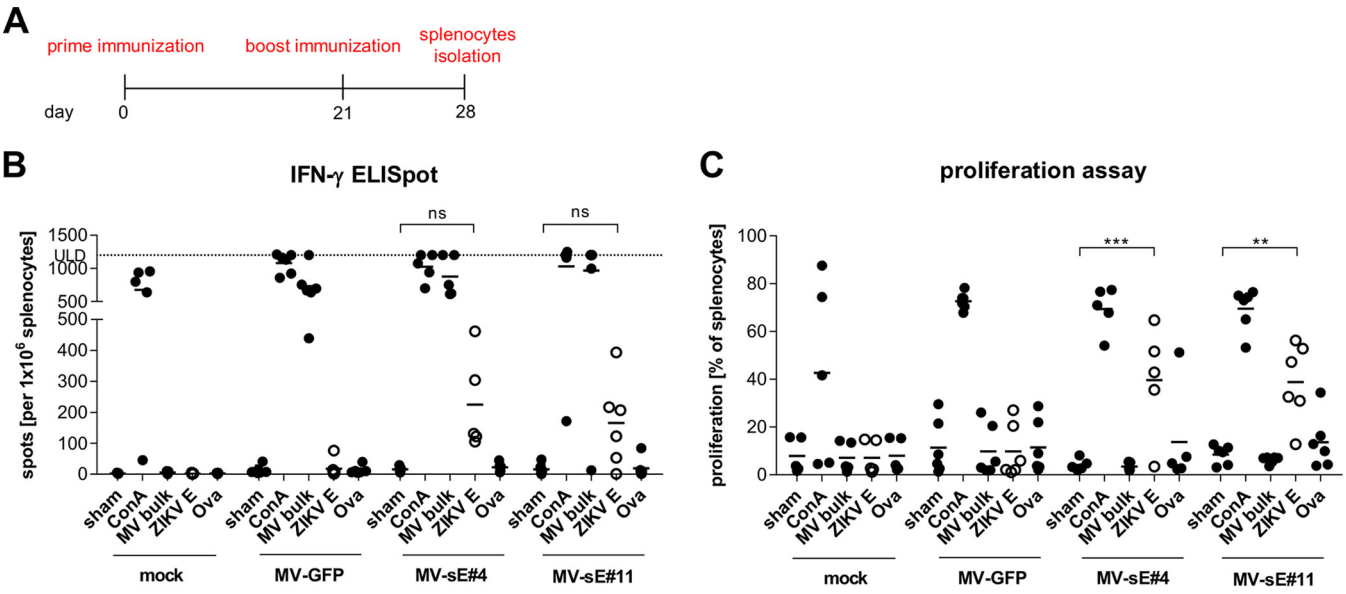

FIG 3 Cellular immune responses induced by recombinant MV. (A) IFNAR$^{-/-}$-CD46Ge mice ($n = 5$ or 6) were immunized with 5×10^4 $TCID_{50}$ of the ZIKV vaccine clone MV-sE#4 or MV-sE#11, MV-GFP control virus, or medium (mock) on days 0 and 21. Seven days after the boost, splenocytes were isolated for analysis of T cell responses. (B) Numbers of IFN-γ-secreting T cells after antigen-specific restimulation were determined by ELISpot analysis using the indicated stimuli: medium (sham), ConA, MV bulk antigen (MV bulk), recombinant ZIKV E protein (ZIKV E), or ovalbumin (Ova). The upper limit of detection (ULD) was 1,200 spots. (C) Proliferation of splenocytes upon restimulation was analyzed by proliferation assay. Individual mouse samples are shown, and the horizontal bars indicate means within each treatment group. ZIKV E-specific responses are represented by open circles. The horizontal lines indicate mean values. Paired two-way ANOVA with Tukey multiple comparison was used for statistics. ns, not significant; **, $P < 0.01$; ***, $P < 0.001$.

against MV of about 400 to 800 VNT. Mock-vaccinated mice did not show MV-specific antibodies. Thus, immunization with both MV-sE vaccine clones robustly induced ZIKV E protein-specific IgG that conferred neutralizing activity against ZIKV while still inducing humoral anti-measles virus immunity similar to that induced by standard MV vaccines.

ZIKV E protein-specific cellular immune responses are also induced by recombinant MV-Zika-sE. To analyze the extents of cellular immune responses, IFNAR$^{-/-}$-CD46Ge mice ($n = 5$ or 6) were vaccinated as described above. Seven days after the boost, the vaccinated mice were euthanized to isolate splenocytes (Fig. 3A). The cells were then restimulated with the specified antigens, and the number of gamma interferon (IFN-γ)-releasing cells was monitored by enzyme-linked immunospot (ELISpot) analysis. The splenocytes of all but two mice revealed similar general reactivities exceeding 500 spots per 1×10^6 splenocytes after stimulation with concanavalin A (ConA), and cells from all but one MV-immunized animal exceeded 500 spots per 1×10^6 splenocytes after restimulation with MV bulk antigen, as well. In contrast, only cells from mice vaccinated with MV-Zika-sE produced IFN-γ upon restimulation with ZIKV E protein, yielding means of 200 and 160 spots per 1×10^6 splenocytes for MV-sE#4 and MV-sE#11, respectively, while no reactivity to control stimulation using ovalbumin was observed.

To gain further evidence for functionality of the splenocytes, T cell proliferation was assessed upon stimulation with the respective antigens (Fig. 3C). At least 50% of splenocytes proliferated after general stimulation with ConA, whereas only 3 to 11% proliferated after sham stimulation and 8 to 13% after control peptide restimulation. In splenocytes isolated from MV-Zika-sE-vaccinated mice, around 40% of splenocytes proliferated after stimulation with ZIKV E protein, while splenocytes of mock- or MV-GFP-vaccinated mice showed no reactivity above unspecific control stimulation. Restimulation with MV bulk antigen did not specifically induce proliferation, most likely due to the inhibitory effect of MV F and H proteins, abundant in the MV bulk antigen preparation, on lymphocyte proliferation (31). Taken together, the data show that bivalent MV/ZIKV vaccine candidates induced not only the expected ZIKV E protein-

specific antibodies with neutralizing activity, but also robust ZIKV E protein-specific cellular immune responses. Moreover, cellular anti-MV responses were similar for MV-Zika-sE and MV-GFP, indicating that robust anti-measles virus immunity was still induced by the bivalent MV/ZIKV vaccine.

Mice are protected from ZIKV challenge. To compare the efficacy of the bivalent MV/ZIKV vaccine candidate to mimic standard flavivirus vaccines with that of an inactivated ZIKV prototype vaccine (i.e., ZPIV), female IFNAR$^{-/-}$-CD46 mice ($n = 16$ or 17) were immunized twice with the respective vaccine, MV-sE#11; vector control, MV-GFP; ZPIV ($n = 6$); or medium (mock) in a prime-boost setup as described above (Fig. 4A). Due to similar immune responses induced by both MV/ZIKV vaccine candidates in the previous experiments, additional inclusion of MV-sE#4 in this *in vivo* experiment was considered redundant. ZIKV E protein-binding antibodies (Fig. 4B) and MV-specific VNT (Fig. 4C) were quantified at 21 days postboost to confirm successful immunization. Vaccination with the bivalent MV-sE induced ZIKV E protein-specific IgG at levels around 1,400 U/ml, whereas vaccination with ZPIV resulted in titers around 270 U/ml (Fig. 4B). As expected, all but one MV-vaccinated mouse developed robust MV-specific neutralizing antibodies (Fig. 4C).

Three weeks after the boost, the mice were mated with BALB/c males to generate allogeneicity of pups in pregnant mice to better mimic the immune status of fetuses in (only) haploidentical mothers. The pregnancy of plug-positive dams was monitored by weight gain (Fig. 4D), and mice presumed to be pregnant were infected with 1×10^3 $TCID_{50}$ ZIKV (strain PF/2013/251013-18) 7 days after a positive plug check. ZIKV plasma viremia was monitored every other day starting day 1 after infection until euthanasia on day 8. Blood, brains, spleens, livers, uteri, or placentas and fetuses were collected, evaluated for pathological changes, and analyzed for prevalence of ZIKV RNA.

Dams immunized with the bivalent MV/ZIKV vaccine candidate gained weight at the same rate as noninfected pregnant control mice (Fig. 4D). In contrast, mock-immunized animals or mice immunized with ZPIV or MV-GFP control showed a statistically significant delay in weight gain (Fig. 4D). At the end of the experiment, splenomegaly was observed in mice vaccinated with MV-GFP or ZPIV or mock vaccinated animals, resulting in an approximately 3-fold higher spleen weight than in uninfected control mice or animals vaccinated with the bivalent MV/ZIKV vaccine candidate (Fig. 4E). Thus, mice vaccinated with MV-sE but not ZPIV had been protected against pathological changes observed in ZIKV-infected, but naive or control-vaccinated mice.

Viremia in the plasma of ZIKV-infected mice was analyzed by quantitative PCR (qPCR) (Fig. 4F and G) using the WHO international ZIKV RNA standard for normalization. Among mock-vaccinated control animals, ZIKV genomes were detected in a single animal 1 dpi (Fig. 4G), and other than a single animal that stayed negative throughout the experiment, all the animals had detectable plasma viremia at 3 dpi, which peaked at 5 dpi and was still above the limit of detection in half of the animals at 8 dpi, the day of sacrifice. No impact of pregnancy on plasma viremia levels was observed in our setting, when pregnant animals were compared to nonpregnant animals (Fig. 4G, dashed lines). Mice immunized with MV-GFP and ZPIV-immunized mice showed comparable kinetics of plasma viremia in both timing and absolute genome copy numbers. In contrast, 9 out of 17 mice immunized with the bivalent MV/ZIKV vaccine candidate MV-sE stayed below the limit of detection. In most of the remaining animals, viral RNA was detected only on day 5 postinfection, with peak ZIKV genome copy numbers about 1 or 2 log units lower than in the other groups. Interestingly, there was no obvious inverse correlation among mice immunized with MV-sE between the levels of ZIKV E protein-binding IgG and the appearance of viremia (data not shown). Moreover, ZIKV RNA was found in spleens, brains, livers, and uteri of the majority of mock- or MV-GFP-vaccinated mice, but also in ZPIV-immunized animals (Fig. 4H to K), with a mean of approximately 10^4 to 10^5 IU ZIKV RNA per 30 mg tissue in spleen or brain and $10^{3.5}$ copies per 30 mg tissue in the liver. Absent or low ZIKV viremia in the tissues of a few individual animals in these groups may be explained by the late time point at day

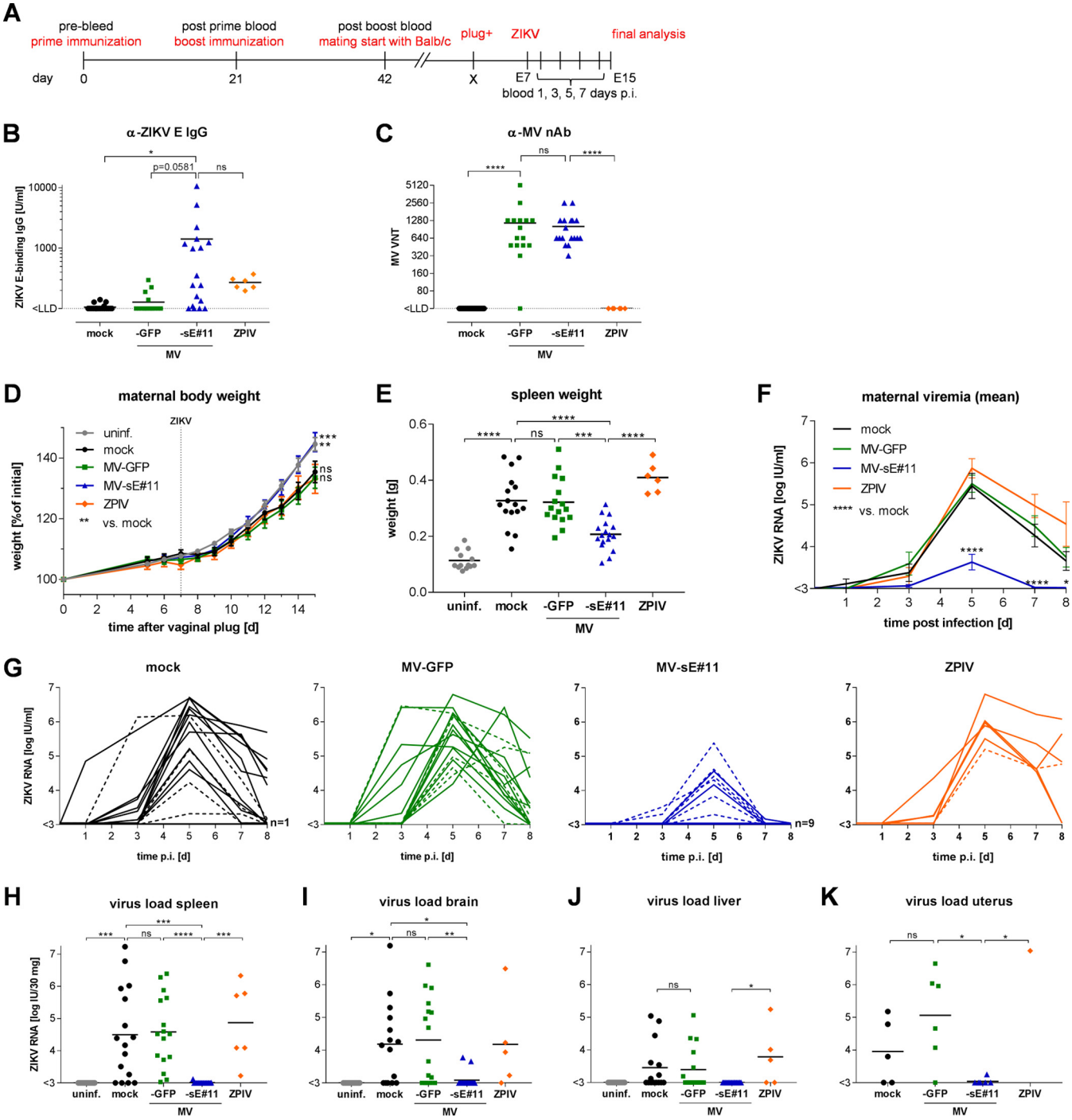

FIG 4 Viremia and ZIKV organ load are reduced in MV-sE#11-vaccinated mice after ZIKV infection. (A) Schematic depiction of vaccination schedule and subsequent steps of ZIKV challenge experiments. In three independent experiments, 16 or 17 female IFNAR$^{-/-}$-CD46Ge mice per group were vaccinated with medium (mock) as a negative control, with 5×10^4 $TCID_{50}$ of MV-sE#11 or MV-GFP, or with a purified inactivated ZIKV preparation (ZPIV; tested in a single replicate experiment; $n = 6$) on days 0 and 21. E, embryonic day. (B and C) ZIKV E-specific IgG levels determined by ELISA (B) and MV VNT (C) were analyzed after boost vaccination. (D and E) Weight curves (D) and spleen sizes (E) of pregnant mice mated at least 21 days postvaccination and challenged at E7.5 reveal symptoms of ZIKV infection in naive mice. One naive control animal was excluded from analysis due to a hematological disorder. (F and G) Plasma viremia of challenged animals determined by ZIKV serum RNA copy numbers of means of different groups (F) or individual animals (G) displayed in the spider blots on days 0, 3, 5, 7, and 8 after ZIKV infection. The dashed lines in panel G indicate serum copy numbers in individual nonpregnant animals. (H to J) ZIKV RNA loads in the indicated organs of challenged animals harvested 8 days after ZIKV challenge or from uninfected dams serving as healthy naive controls (uninf.). (K) Analysis of uteri of nonpregnant mice. Animals vaccinated with MV-sE#11 are depicted in blue, MV-GFP in green, ZPIV in orange, mock-vaccinated animals in black, and uninfected naive controls in gray. The horizontal lines indicate mean values; the error bars represent standard errors of the mean. Statistical analysis was by two-way (B to D and F) or one-way (E and H to K) ANOVA with Tukey multiple comparison. ns, not significant; *, $P < 0.05$; **, $P < 0.01$; ***, $P < 0.001$; ****, $P < 0.0001$.

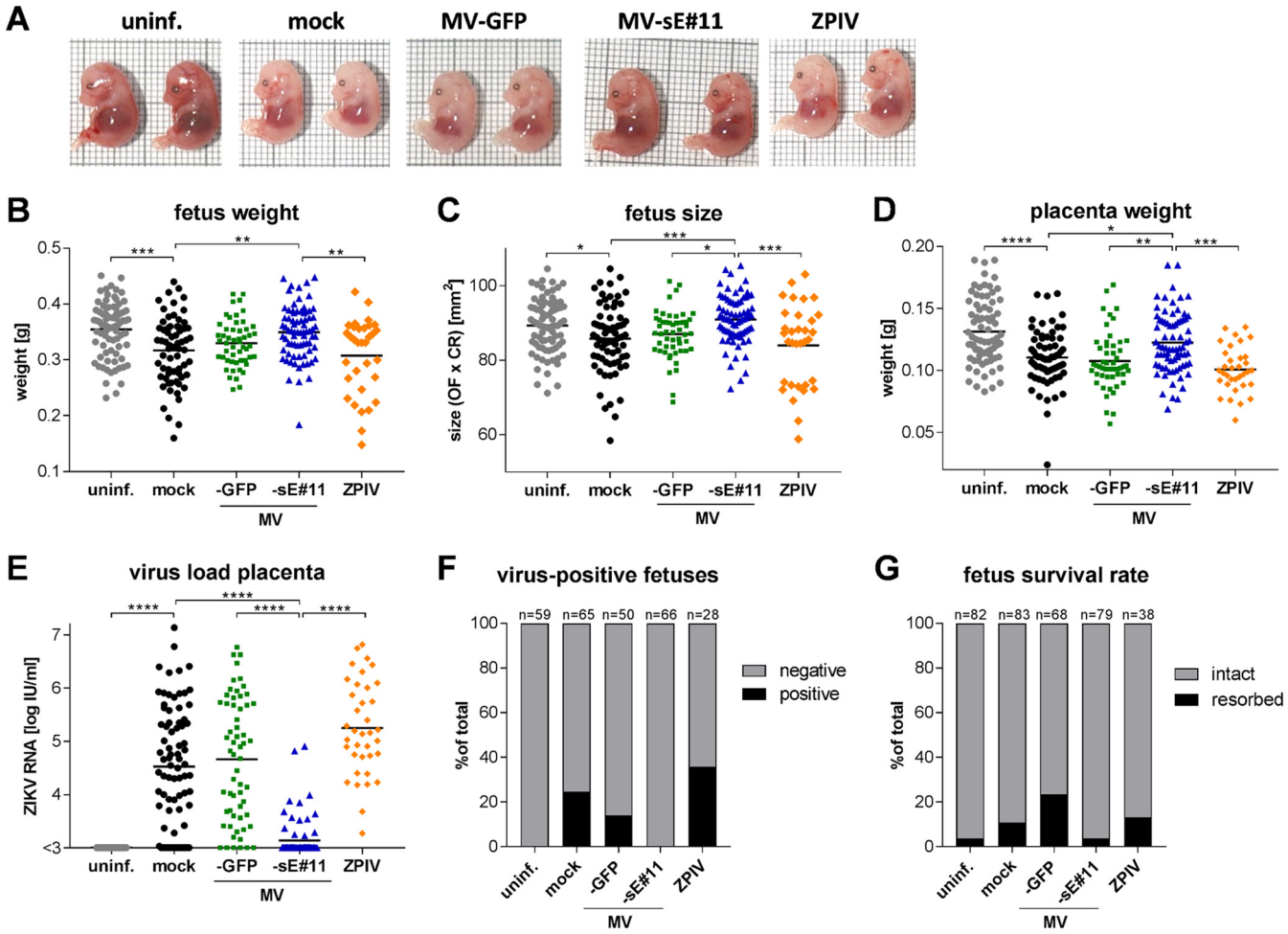

FIG 5 Fetuses from MV/ZIKV-vaccinated pregnant mice are protected during ZIKV challenge. Fetuses of challenged pregnant dams shown in Fig. 4 were harvested and analyzed for phenotypic changes. (A) Representative images of two E15.5 fetuses each from different groups at time of harvest. (B to D) Fetus weight (B) and size (determined as crown-to-rump length times the occipitofrontal diameter of the head) (C), as well as placental weight (D). (E and F) ZIKV RNA copy numbers in a 30-mm³ piece of placenta (E) and signals for ZIKV RNA above the limit of detection (1×10^2 copies) in fetus heads (F) determined by quantitative PCR. (G) Resorption rates in dams after ZIKV challenge indicate fetal demise. Animals vaccinated with MV-sE are depicted in blue, MV-GFP in green, ZPIV in orange, mock-vaccinated animals in black, and uninfected naive controls in gray. One uninfected animal (same as in Fig. 4) and her fetuses were excluded from analysis due to a hematological disorder. (B to E) The horizontal lines indicate mean values. Statistical analysis was by one-way ANOVA with Tukey multiple comparison. *, $P < 0.05$; **, $P < 0.01$; ***, $P < 0.001$; ****, $P < 0.0001$.

8 postinfection, when the samples were taken. At that time, blood viremia had also dropped significantly, in some animals even below the limit of detection. However, in mice vaccinated with the bivalent MV/ZIKV vaccine candidate MV-sE, ZIKV RNA was found in the brains of only two animals (Fig. 4I) and in the spleen and uterus of one animal after challenge with ZIKV (Fig. 4H and K). No ZIKV RNA was detected in the liver of any mouse vaccinated with MV-sE (Fig. 4J). In conclusion, vaccination with MV-sE significantly reduced infection levels in mice challenged with ZIKV, in more than half of the animals even below the limit of detection, while vaccination with ZPIV had no clear beneficial effect.

Fetuses of dams vaccinated with the bivalent MV/ZIKV vaccine candidate MV-sE are protected from ZIKV. Gross pathological examination of the fetuses from the challenge experiment revealed different pathological changes. ZIKV infection of pregnant mock- or MV-GFP-vaccinated dams resulted in fetuses smaller and paler (Fig. 5A) than fetuses of noninfected controls (Fig. 5A, uninf.), indicating intrauterine growth retardation and possibly anemia. Fetuses from dams vaccinated with the bivalent MV/ZIKV vaccine candidate MV-sE (Fig. 5A) looked comparable to uninfected controls, whereas fetuses of dams vaccinated with ZPIV (Fig. 5A) were as pale and small as

fetuses of infected, mock-vaccinated dams. In addition, a considerable number of fetuses had died and were subsequently resorbed in control- or ZPIV-vaccinated animals (Fig. 5G). In contrast, this was only rarely observed in uninfected controls or animals vaccinated with the bivalent MV/ZIKV vaccine candidate MV-sE. To quantify these observations, fetus weight and size were analyzed (Fig. 5B and C). Vaccination of dams with the bivalent MV/ZIKV vaccine candidate MV-sE protected fetuses from the growth retardation observed in control- and ZPIV-vaccinated animals. This effect correlated with the weight of the associated placentas and inversely with their ZIKV loads (Fig. 5D and E). ZIKV infection of mock-, MV-GFP-, and ZPIV-immunized dams resulted in significantly reduced placenta weight and high viral loads, with the viral load in the ZPIV group even reaching slightly higher titers. In contrast, placentas from dams vaccinated with the bivalent MV/ZIKV vaccine candidate MV-sE were similar to those of uninfected dams. Moreover, vaccination of dams with MV-sE strongly reduced the viral load in the placenta, with only 14 out of 71 placentas becoming positive for ZIKV RNA at all (Fig. 5E), and no viral RNA became detectable in any fetal heads (Fig. 5F). On the other hand, all placentas of ZPIV-vaccinated dams and of the vast majority of control group dams had detectable ZIKV RNA titers after challenge, also reflected in a remarkable number of fetus heads with detectable ZIKV RNA, indicating transplacental infection in these groups. Thus, while ZIKV infection was highly teratogenic in the control groups, as well as the ZPIV-immunized animals, vaccination of dams with the bivalent MV/ZIKV vaccine candidate MV-sE resulted in robust protection of fetuses.

DISCUSSION

In this study, we aimed to compare the efficacies of an MV-derived vaccine candidate, MV-Zika-sE, and a prototypic inactivated flavivirus vaccine preparation to protect against the teratogenic sequelae of ZIKV infection. We showed that MV-Zika-sE replicated with MV vaccine strain-like characteristics, induced robust humoral and cellular immune responses directed against the ZIKV envelope (E) protein, and was protective in an *in vivo* challenge model of pregnant mice. MV-Zika-sE-immunized mice experienced significantly milder or no clinical signs, such as reduced weight gain or splenomegaly, after ZIKV challenge. We also observed significantly lower peak titers and shorter duration of systemic viremia, as well as reduced or no virus loads in brain, spleen, liver, and placenta/uterus. More than half of the immunized mice were completely protected from ZIKV infection, as illustrated by absence of viremia. *In utero* transmission of ZIKV from MV-Zika-sE-immunized dams to their fetuses remained below the limit of detection, and fetuses showed normal growth with no evidence of other teratogenic effects. In contrast, inactivated alum-adjuvanted ZIKV vaccine resulted in antibody induction in vaccinated animals but did not confer protection after challenge.

The protective MV Schwarz strain-derived recombinant vaccine MV-Zika-sE is a live-attenuated vaccine that encodes a soluble version of the ZIKV E protein as the main target for functional antibodies, but potentially also T cell responses. Vero cells revealed homogeneous expression of the ZIKV E antigen by Western blot analysis and positive immunostaining of syncytia after infection by MV-Zika-sE (Fig. 1B and C). Stable antigen expression by the recombinant vaccine is prerequisite, as the immune system must encounter this antigen to mount robust specific immune responses (32), and has been described previously for a considerable number of similarly constructed MV vaccine strain-derived candidates targeting additional pathogens (26). Also, a number of antigens from other pathogens, including flaviviruses (27–29) and even *Helicobacter pylori* (33), have been among the targets, revealing the broad applicability of MV as a vaccine platform. Thus, MV-derived vaccines take advantage of the live-attenuated nature of the MV-derived backbone, which is a powerful immune stimulator triggering both humoral and cellular responses against homologous, as well as heterologous, antigens (34). Moreover, the natural tropism of vaccine strain MV for lymphatic cells, including professional antigen-presenting cells (35), most likely acts as a boost.

The ZIKV vaccine candidates under investigation are based on either direct vaccination with E protein, expression of E protein, or viral particles (36). Among them, ZPIV

(37) has already demonstrated its efficacy. The failure of ZPIV observed in our experiments was likely due to the overall very low IgG titers induced. In the former study (37), only titers above a certain threshold (ZIKV E IgG $>$ 10^3 U/ml) were found to be protective, whereas animals with 10-fold lower titers, similar to those observed here, were not protected against infection (37). However, in MV-Zika-sE-vaccinated mice with similarly low antibody titers, viremia in plasma and several organs was consistently lower than in ZPIV-vaccinated animals. Other factors, possibly cellular immune responses induced by the MV-Zika-sE vaccine, likely account for these differences, thereby contributing to protection against ZIKV challenge.

This protective effect of MV-Zika-sE, especially during pregnancy, was demonstrated after a standard prime-boost vaccination in an adapted allogeneic mouse model. From our data, we can neither exclude nor conclude that there were already protective effects after the prime vaccination, when we could detect antibody responses that were boosted about 5-fold after the second vaccination. These analyses require further investigations in a dedicated experimental setting, since the implications for the practical use of the vaccine candidate will be considerable, but these are beyond the scope of our current study. For the challenge model, we used MV receptor-transgenic IFNAR$^{-/-}$-CD46Ge mice in a C57/BL6 background, the long-accepted small animal model for MV vaccines (38), as dams. One potential limitation of this mouse strain for analyzing immunity induced by MV-derived vaccines may be found in the deficiency of the mice, and especially their immune cells, in reacting to type I interferons. Usually, type I interferons are regarded as quite crucial for cross-linking innate and adaptive immune responses and for effective induction of the latter. Consequently, use of these mice may result in an underestimation of the immunogenicity of MV-derived vaccines, but that would not affect our general conclusions. Interestingly, the presence of human CD46 (hCD46) has recently been shown to be dispensable in overcoming the host restriction of MV in mice (39), and thus, use of IFNAR knockout mice alone would have been sufficient for testing the recombinant MV/ZIKV vaccine candidates, while deficient IFN reactivity is also needed for the ZIKV challenge model.

After vaccination in the standard regimen (32), immunized females were mated with BALB/c males to mimic the natural genetic heterozygosity between mothers and fetuses. A similar system has been successfully applied to assess the effects of influenza A virus infection on unborn offspring (40) and most recently also for the effects of intrauterine ZIKV infection on newborn animals and their development (41). Challenging these pregnant mice revealed the teratogenic effects of ZIKV infection, including the intrauterine growth retardation observed previously in a model that also takes advantage of the heterozygous IFN-α/β receptor status of pups in IFNAR-deficient dams and a closely related challenge virus, ZIKV strain H/PF/2013 (42). Besides growth retardation, we observed two other effects of ZIKV infection in our model: splenomegaly and a putative anemic phenotype of fetuses. The latter has been reported before and was described as "pallor" (42). In addition, recent analyses of fetal blood samples from ZIKV-infected mothers also revealed anemia (43), warranting further investigation of the underlying mechanisms.

In this study, we took advantage of the recently developed WHO reference standard (44), allowing us to quantify viral RNA copy numbers in standardized units. This method of standardization enables direct cross-comparison of our model and results to other studies using the same readily available standard. Although it was intentionally developed for the most desirable worldwide standardization of outcomes of clinical studies and trials, the standard is also of value for preclinical studies and ZIKV research in general.

In conclusion, the bivalent MV/ZIKV vaccine candidate has a number of desirable properties with respect to its immunogenicity and protective capacity against ZIKV infection. Furthermore, the concurrent induction of anti-MV immunity would allow its use in the context of routine measles immunization schedules. Such an MV-based ZIKV vaccine could be included in the currently applied MMR (measles, mumps, rubella) vaccine, providing protection against two teratogenic infections, ZIKV and rubella. Children and adolescents

would be vaccinated before puberty, and women would develop robust immunity before pregnancy, as already accomplished for rubella. Therefore, MV-Zika-sE is a promising vaccine candidate that warrants further investigation.

MATERIALS AND METHODS

Cells. Vero (African green monkey kidney; ATCC CCL-81) cells were purchased from the ATCC (Manassas, VA, USA). Vero cells were cultured in Dulbecco's modified Eagle's medium (DMEM) supplemented with 10% fetal bovine serum (FBS) (Biochrom, Berlin, Germany) and 2 mM L-glutamine (Biochrom) at 37°C in a humidified atmosphere with 6% CO_2 for no longer than 6 months after thawing of the original stock.

Recombinant MV-Zika-sE vaccine clones. A prototypic MV-based vaccine targeting ZIKV and consisting of recombinant Schwarz strain-derived MV encoding soluble E protein of ZIKV was purchased from Themis Biosciences GmbH (Vienna, Austria), who cloned and generated the vaccine clones. In short, the gene encoding the sequence of ZIKV E protein (strain BeH818995; GenBank accession no. KU365777.1) was modified to be expressed in a soluble form by deleting the whole stem-anchor region via truncation of the open reading frame at nucleotide 2184 of the viral genome. The ZIKV genes encoding prM, including the preceding SP, encompassed by the last 18 amino acids of C and the modified sE, were codon optimized (Eurofins Genomics, Ebersberg, Germany), and a Kozak sequence was added in front of the SP-prM genes. The whole sequence was generated by gene synthesis (Eurofins Genomics). The synthetic gene was inserted into the recombinant measles virus Schwarz strain backbone plasmid (45) in an additional transcription cassette following the P gene cassette using restriction enzymes BsiWI and BssHII. Recombinant MV was rescued as previously described (46). 293-3-46 cells stably expressing T7 polymerase and the MV proteins N and P were transfected with the recombinant MV genomes and a plasmid encoding MV polymerase L. Vero 10-87 cells were overlaid with transfected 293-3-46 cells, and single syncytia were picked and further passaged up to passage 8. The GFP-encoding control vaccine MV_{Schw}-GFP has been described previously (45).

Virus. To amplify ZIKV isolate PF13/251013-18 (47), Vero cells were seeded in T175 flasks and infected at a confluence of 70% and an MOI of 0.001 in 10 ml serum-free DMEM containing 2 mM L-glutamine for 2 h at 37°C. After removal of the inoculum, 40 ml of DMEM containing 2 mM L-glutamine and 2% FBS was added, and the culture was incubated at 37°C, 6% CO_2 in a humidified atmosphere. ZIKV-containing cell supernatant was harvested when 70% of the cells were detached due to the viral cytopathic effect. Cellular debris was removed by centrifugation, and the virus was subsequently stored at −80°C in aliquots.

Virus titration. The titers of recombinant MV and ZIKV were determined by the $TCID_{50}$ method of Kaerber and Spearman (48, 49). Vero cells were infected with 10-fold serially diluted virus suspensions and cultivated for 3 to 5 days to determine wells showing syncytia derived from MV infection or 6 days for determination of wells containing Vero cells showing cytopathic effect due to ZIKV infection.

Preparation of formalin-inactivated ZIKV vaccine. For preparation of the formalin-inactivated ZIKV particle vaccine (ZPIV), a virus suspension was loaded onto a 20% sucrose cushion and pelleted at 25,000 rpm for 2 h at 4°C (SW28 rotor; Beckmann Coulter, Pasadena, CA). Serum proteins were removed from the virus pellet resuspended in 150 μl phosphate-buffered saline (PBS) as described previously (50) using Capto Core 700 slurry (GE Healthcare, Chicago, IL). In short, Capto Core 700 slurry was washed 3 times with PBS; 1 ml washed slurry was mixed with 1 ml PBS, and 250 μl of this suspension was mixed with 900 μl virus suspension for 1 h at room temperature. After incubation, the suspension was centrifuged at 800 × *g* for 5 min, and supernatant containing purified virus was used for formalin inactivation. Purified ZIKV was inactivated with 0.05% formalin (37%) for 24 h at 37°C. To remove excess formalin from inactivated ZIKV, a two-step dialysis against PBS was performed at 4°C for 7 h and 20 h using Slide-A-Lyzer dialysis cassettes (Thermo Fisher Scientific, Bremen, Germany) with a 10-kDa cutoff loaded with 100 μl inactivated virus suspension. Before vaccination, formalin-inactivated ZIKV particles normalized to 1 μg ZIKV E protein per mouse were extensively mixed with 500 μg $Al(OH)_3$ (Alhydrogel adjuvant 2%; catalog no. mvac-alu-250; Invivogen) by pipetting for 5 min in 150 μl (total volume) Opti-MEM. This mixture was incubated for approximately 30 min at room temperature before application.

Western blot analysis. For Western blot analysis, Vero cells cultured in 6-well dishes were lysed 2 days postinfection (MOI = 0.1) and immunoblotted as previously described (51). A polyclonal rabbit anti-ZIKV envelope protein antibody (1:10,000; GTX133314; GeneTex, Irvine, CA) was used as the primary antibody for ZIKV E protein and a rabbit anti-MV N polyclonal antibody (1:25,000; Abcam, Cambridge, United Kingdom) for MV N. A horseradish peroxidase (HRP)-coupled donkey anti-rabbit IgG(H+L) polyclonal antibody (1:10,000; Rockland, Gilbertsville, PA) served as the secondary antibody. Peroxidase activity was visualized with an enhanced chemiluminescence detection kit (Thermo Scientific) with the detection system MicroChemi 4.2 (DNR Bio Imaging System, Neve Yamin, Israel).

Immunoperoxidase monolayer assay. For immunoperoxidase monolayer assay analysis, Vero cells cultured in flat-bottom 96-well plates were fixed overnight with ethanol (−20°C) 2 days postinfection (MOI = 0.05). For staining, the fixed cells were washed 3 times with 1 ml PBS and subsequently blocked with PBS plus 2% bovine serum albumin (BSA) (Roth, Karlsruhe, Germany) for 30 min at 37°C. The cells were then probed for 1 h with a polyclonal rabbit anti-ZIKV envelope protein antibody (1:1,000; GTX133314; GeneTex) or a rabbit anti-MV N polyclonal antibody (1:1,000) in PBS plus 2% BSA. The cells were washed 3 times with 1 ml PBS and subsequently probed with the secondary HRP-coupled donkey anti-rabbit IgG(H+L) polyclonal antibody (1:1,000; Rockland) for 1 h at 37°C. Then, the cells were washed 3 times again. For detection, the cells were stained with TrueBlue peroxidase substrate solution (SeraCare, Milford, MA, USA).

Animal experiments. All animal experiments were carried out in compliance with the regulations of the German animal protection law and were authorized by the RP Darmstadt, Hesse, Germany. Six- to 12-week-old IFNAR$^{-/-}$-CD46Ge mice with knockout of the type I interferon receptor and heterozygous for human CD46 (38) were immunized in a prime-boost setup on days 0 and 28. The mice were vaccinated via the intraperitoneal (i.p.) route with either 5×10^4 $TCID_{50}$ of recombinant MV (in a 200-μl total volume), 200 μl Opti-MEM (mock), or subcutaneously (s.c.) with formalin-inactivated ZPIV normalized to 1 μg ZIKV E protein in a total volume of 150 μl. Blood was collected from the tail or the submandibular vein on days 0 and 28, and the serum was stored at −20°C. For antibody analysis, mice were euthanized on day 49, and serum samples were prepared and stored at −20°C. For analysis of cellular immune responses, mice were vaccinated as described above, and spleens were isolated on day 35. For challenge experiments, female IFNAR$^{-/-}$-CD46Ge mice were vaccinated as described above, and 21 days after the boost vaccination, the vaccinated mice were mated allogeneically with male BALB/c mice in a 1:2 or 1:1 scheme for one night (40). Successful mating was verified by plug check on the following day. Plug-positive mice were infected 8 days postmating with 1×10^3 $TCID_{50}$ of ZIKV strain PF/2013/251013-18 applied s.c. in 100 μl Opti-MEM. The mice were checked daily for appearance of symptoms, and 20 μl blood was drawn 1, 3, 5, and 7 days postinfection from the submandibular vein. Serum was stored at −20°C. On day 8 postinfection, the mice were euthanized and blood was sampled. Furthermore, selected organs (brain, spleen, liver, uterus, and placentas) and fetuses were prepared, documented, weighed, shock frozen in liquid nitrogen, and stored at −80°C.

Antibody ELISA. A Recombivirus mouse α-Zika virus envelope protein IgG ELISA kit was purchased (Alpha Diagnostic International, San Antonio, TX) and used according to the manufacturer's instructions at room temperature. In brief, serum samples diluted 1:100 or 1:500 in low-NSB sample diluent (LNSD) buffer provided within the ELISA kit from mice euthanized 3 weeks after boost and controls were added in duplicate to the provided prewashed 96-well plates coated with immobilized ZIKV E protein. After 1 h of incubation, the plates were washed 4 times, and anti-mouse IgG HRP-coupled antibody was added for 30 min, followed by 5 washing steps. Then, 100 μl of 3,3′,5,5′-tetramethylbenzidine (TMB) substrate solution provided within the kit was added for 15 min, followed by addition of 100 μl stop solution. The optical density (OD) was measured at 450 nm with a reference wavelength of 630 nm (Tecan Sunrise, Männedorf, Switzerland).

Determination of neutralizing antibody titers. The quantification of VNT targeting MV was done as previously described (52). Duplicates of mouse sera were serially diluted in 2-fold dilutions in DMEM, and 50 PFU of MV_{vac2}-GFP(P) (53) were added to the serum dilutions and incubated for 1 h at 37°C. The virus-serum suspensions were added to 1×10^4 Vero cells seeded 4 h prior to the assay in 96-well plates, and the infected cultures were incubated for 4 days at 37°C. VNT were calculated as the reciprocal of the highest serum dilution completely abolishing infection. For determination of ZIKV neutralizing antibodies, PRNTs were determined. Duplicates of mouse sera were 2-fold serially diluted in Opti-MEM, and 50 μl DMEM containing 100 $TCID_{50}$ ZIKV was added per well and incubated at 37°C for 1 h. Then, the virus-serum mixture was added to 2×10^6 Vero cells seeded per 10-cm dish on the previous day and incubated for another 2 h at 37°C, after which the inoculum was removed and the cells were overlaid with a final concentration of 0.8% low-melting-point agarose in 10 ml complete DMEM. For assay readout, the agarose overlay was carefully removed 6 days after infection, and the cells were fixed with 4% formalin in PBS and then stained with 0.1% crystal violet to visualize plaques in the confluent cell layer. The $PRNT_{50}$ was determined as the reciprocal of the serum dilution leading to at least 50% reduction in plaque numbers relative to a plate incubated with ZIKV without addition of neutralizing serum.

ELISpot analysis. Murine IFN-γ ELISpot assays were purchased (eBioscience, Frankfurt, Germany) and performed according to the manufacturer's instructions. Splenocytes (5×10^5) isolated 7 days postinfection were cocultured for specific restimulation for 36 h in 200 μl RPMI 1640 medium (10% FBS, 2 mM L-Gln, 1% penicillin-streptomycin) containing the antigen(s) of interest in Multiscreen-IP ELISPOT polyvinylidene difluoride (PVDF) 96-well plates (Millipore, Darmstadt, Germany). The splenocytes were restimulated with either 10 μg/ml ZIKV E protein (Creative Diagnostics, Shirley, NY) or 10 μg/ml ovalbumin as the protein control. Medium served as a mock control; 10 μg/ml ConA (Sigma-Aldrich, St. Louis, MO) was used to ensure the splenocytes' general reactivity, and 10 μg/ml recombinant MV bulk antigens (Virion Serion, Würzburg, Germany) was used to determine MV-specific cellular immune responses. Afterward, the stimulated splenocytes were removed, and the plates were incubated with biotin-conjugated anti-IFN-γ antibodies and subsequently with avidin-HRP according to the manufacturer's instructions. AEC (3-amino-9-ethyl-carbazole) substrate solution was prepared according to the manufacturer's instructions using 3-amino-9-ethyl-carbazole (Sigma-Aldrich) dissolved in *N*,*N*-dimethylformamide (Merck Millipore, Burlington, MA) and used for signal detection. Spots were counted using an Eli.Scan ELISpot scanner (A.EL.VIS, Hamburg, Germany) and ELISpot analysis software (A.EL.VIS). Wells with too many spots to be separated were set to >1,200 spots (the maximum spot count reliably determined).

T cell proliferation assay. Splenocytes isolated 1 week after the boost were labeled with 0.5 μM carboxyfluorescein succinimidyl ester (CFSE) (eBioscience) as previously described (54). Labeled cells (5×10^5) were seeded in RPMI 1640 supplemented with 10% mouse serum, 2 nM L-glutamine, 1 mM HEPES, 1% penicillin-streptomycin, and 100 μM 2-mercaptoethanol in 96-well plates and restimulated as described previously (52) with ConA (10 μg/ml), MV bulk antigens (10 μg/ml), or Zika E protein (10 μg/ml), and the cells were cultured for 6 days. Medium or ovalbumin (10 μg/ml) served as controls. The cells were fixed with 1% paraformaldehyde in PBS and analyzed by flow cytometry using an LSR II flow cytometer (BD) and FACSDiva software (BD).

RNA preparation. For purification of viral RNA from mouse serum, the QIAamp viral RNA Mini kit (Qiagen, Hilden, Germany) was used, and for purification of RNA from organ tissue, an RNeasy Plus Mini kit

(Qiagen) was used according to the manufacturer's instructions. In brief, 10 μl of serum sample was diluted in a total volume of 140 μl PBS, and RNA was eluted from the column with 60 μl AVE buffer. About 30 μg of frozen tissue samples was homogenized in 600 μl RLT Plus buffer in 2 ml Lysing Matrix D tubes (MP Bioscience, Hilton, UK) containing 1.4-mm ceramic spheres using a Precellys 24 homogenizer (MP Bioscience) for 10 s at 5,000 rpm. As an RNA preparation control, tissue and serum samples were spiked before RNA extraction with the external equine arteritis virus (EAV) RNA provided in the LightMix Modular EAV RNA extraction control 660 kit (TIB Molbiol, Berlin, Germany) for codetection during quantitative multiplex PCR.

Determination of virus genome copy numbers by qPCR. ZIKV RNA, as well as external EAV RNA, was detected in serum samples and tissues via multiplex quantitative reverse transcription-PCR (qRT-PCR) using LightMix modular ZikaV (FAM [6-carboxyfluorescein]) (TIB Molbiol) and a LightMix modular EAV RNA extraction control kit 660 (TIB Molbiol) in combination with a LightCycler multiplex RNA Virus Master (Roche, Basel, Switzerland). qPCRs were performed in a 96-well format with 5 μl of RNA in a total volume of 20 μl run in triplicate on a CFX 96 qPCR cycler (Bio-Rad Laboratories, Hercules, CA). The WHO reference standard (11468/16) of Zika virus RNA (44) was purified similarly to serum samples and was used as an absolute ZIKV RNA standard (in international units per milliliter) during each qPCR (linear range, 10^3 to 10^7 IU/ml). The amount of ZIKV RNA in each sample (in international units per milliliter) was then determined according to the threshold cycle (C_T) value in respect to the standard curve. The cycling conditions were as follows: reverse transcription for 300 s at 55°C, followed by denaturation for 300 s at 95°C, and 45 cycles of 5 s at 95°C, 15 s at 60°C, and 15 s at 72°C. The final cooling step was 30 s at 40°C.

ACKNOWLEDGMENTS

This work was supported by BMG grant 1-2516-FSB-416 (M.D.M. and G.G.) and by the German Center for Infection Research (DZIF) (TTU 01.802 [M.D.M.] and TTU 01.916 [G.G.]).

We thank Carina Kruip, Daniela Müller, Mona Lange, and Arne Auste for excellent technical assistance. We are indebted to Didier Musso and coworkers from Institut Louis Malardé for providing ZIKV isolate PF13/251013-18 and to Roberto Cattaneo for providing the IFNAR$^{-/-}$-CD46Ge mice. We are grateful to Constance Yue for help with setting up the qPCR protocol, as well as to Henning Jacobsen for introduction to the mouse pregnancy model. Moreover, we thank Veronika von Messling for critically reading the manuscript and Sabrina Schrauf for helpful discussions.

REFERENCES

1. Moore CA, Staples JE, Dobyns WB, Pessoa A, Ventura CV, Fonseca EB, Ribeiro EM, Ventura LO, Neto NN, Arena JF, Rasmussen SA. 2017. Characterizing the pattern of anomalies in congenital Zika syndrome for pediatric clinicians. JAMA Pediatr 171:288–295. https://doi.org/10.1001/jamapediatrics.2016.3982.
2. Pan American Health Organization. 2017. Zika-epidemiological report Brazil. https://www.paho.org/hq/dmdocuments/2017/2017-phe-zika-situation-report-bra.pdf.
3. World Health Organization. 2018. List of Blueprint priority diseases. http://www.who.int/blueprint/priority-diseases/en/.
4. World Health Organization/UNICEF. 2017. WHO/UNICEF Zika vaccine target product profile 2016: upate 2017. http://www.who.int/immunization/research/development/zika/en/.
5. Rogers DJ, Wilson AJ, Hay SI, Graham AJ. 2006. The global distribution of yellow fever and dengue. Adv Parasitol 62:181–220. https://doi.org/10.1016/S0065-308X(05)62006-4.
6. Miner JJ, Diamond MS. 2017. Zika virus pathogenesis and tissue tropism. Cell Host Microbe 21:134–142. https://doi.org/10.1016/j.chom.2017.01.004.
7. Dick GWA, Kitchen SF, Haddow AJ. 1952. Zika virus (I). Isolations and serological specificity. Trans R Soc Trop Med Hyg 46:509–520. https://doi.org/10.1016/0035-9203(52)90042-4.
8. Simpson DIH. 1964. Zika virus infection in man. Trans R Soc Trop Med Hyg 58:339–348. https://doi.org/10.1016/0035-9203(64)90201-9.
9. Moore DL, Causey OR, Carey DE, Reddy S, Cooke AR, Akinkugbe FM, David-West TS, Kemp GE. 1975. Arthropod-borne viral infections of man in Nigeria, 1964-1970. Ann Trop Med Parasitol 69:49–64. https://doi.org/10.1080/00034983.1975.11686983.
10. Lanciotti RS, Kosoy OL, Laven JJ, Velez JO, Lambert AJ, Johnson AJ, Stanfield SM, Duffy MR. 2008. Genetic and serologic properties of Zika virus associated with an epidemic, Yap State, Micronesia, 2007. Emerg Infect Dis 14:1232–1239. https://doi.org/10.3201/eid1408.080287.
11. Cao-Lormeau VM, Roche C, Teissier A, Robin E, Berry AL, Mallet HP, Sall AA, Musso D. 2014. Zika virus, French Polynesia, South Pacific, 2013. Emerg Infect Dis 20:1085–1086. https://doi.org/10.3201/eid2006.140138.
12. Musso D, Nhan T, Robin E, Roche C, Bierlaire D, Zisou K, Shan YA, Cao-Lormeau VM, Broult J. 2014. Potential for Zika virus transmission through blood transfusion demonstrated during an outbreak in French Polynesia, November 2013 to February 2014. Euro Surveill 19:20761. https://doi.org/10.2807/1560-7917.ES2014.19.14.20761.
13. Cheng X, Zengel JR, Suguitan AL, Xu Q, Wang W, Lin J, Jin H. 2013. Evaluation of the humoral and cellular immune responses elicited by the live attenuated and inactivated influenza vaccines and their roles in heterologous protection in ferrets. J Infect Dis 208:594–602. https://doi.org/10.1093/infdis/jit207.
14. Gilbert SC. 2012. T-cell-inducing vaccines—what's the future. Immunology 135:19–26. https://doi.org/10.1111/j.1365-2567.2011.03517.x.
15. Darwish MA, Hammon WM. 1966. Japanese B encephalitis virus vaccines from tissue culture. VII. Formalin inactivated Nakayama strain vaccine. Proc Soc Exp Biol Med 122:813–816. https://doi.org/10.3181/00379727-122-31258.
16. Price WH, Thind IS. 1969. Live and inactivated vaccines of group B arboviruses. Role of neutralizing antibody and serum protective factor. Nature 222:1294–1295. https://doi.org/10.1038/2221294a0.
17. Doe B, Selby M, Barnett S, Baenziger J, Walker CM. 1996. Induction of cytotoxic T lymphocytes by intramuscular immunization with plasmid DNA is facilitated by bone marrow-derived cells. Proc Natl Acad Sci U S A 93:8578–8583. https://doi.org/10.1073/pnas.93.16.8578.
18. Corr M, Lee DJ, Carson DA, Tighe H. 1996. Gene vaccination with naked plasmid DNA. Mechanism of CTL priming. J Exp Med 184:1555–1560. https://doi.org/10.1084/jem.184.4.1555.
19. Phillpotts RJ, Venugopal K, Brooks T. 1996. Immunisation with DNA polynucleotides protects mice against lethal challenge with St. Louis encephalitis virus. Arch Virol 141:743–749. https://doi.org/10.1007/BF01718332.
20. Kochel T, Wu SJ, Raviprakash K, Hobart P, Hoffman S, Porter K, Hayes C. 1997. Inoculation of plasmids expressing the dengue-2 envelope gene elicit neutralizing antibodies in mice. Vaccine 15:547–552. https://doi.org/10.1016/S0264-410X(97)00215-6.
21. Theiler M, Smith HH. 1937. The use of yellow fever virus modified by in vitro cultivation modified by in vitro cultivation for human immunization. J Exp Med 65:787–800. https://doi.org/10.1084/jem.65.6.787.
22. Theiler M, Smith HH. 1937. The effect of prolonged cultivation in vitro

upon the pathogenicity of yellow fever virus. J Exp Med 65:767–786. https://doi.org/10.1084/jem.65.6.767.
23. Thomssen R. 1975. Live attenuated versus killed virus vaccines. Monogr Allergy 9:155–176.
24. Tlaxca JL, Ellis S, Remmele RL. 2015. Live attenuated and inactivated viral vaccine formulation and nasal delivery. Potential and challenges. Adv Drug Deliv Rev 93:56–78. https://doi.org/10.1016/j.addr.2014.10.002.
25. Suder E, Furuyama W, Feldmann H, Marzi A, de Wit E. 2018. The vesicular stomatitis virus-based Ebola virus vaccine. From concept to clinical trials. Hum Vaccin Immunother 1–7. https://doi.org/10.1080/21645515.2018.1473698.
26. Mühlebach MD. 2017. Vaccine platform recombinant measles virus. Virus Genes 53:733–740. https://doi.org/10.1007/s11262-017-1486-3.
27. Brandler S, Lucas-Hourani M, Moris A, Frenkiel M-P, Combredet C, Février M, Bedouelle H, Schwartz O, Desprès P, Tangy F. 2007. Pediatric measles vaccine expressing a dengue antigen induces durable serotype-specific neutralizing antibodies to dengue virus. PLoS Negl Trop Dis 1:e96. https://doi.org/10.1371/journal.pntd.0000096.
28. Desprès P, Combredet C, Frenkiel M-P, Lorin C, Brahic M, Tangy F. 2005. Live measles vaccine expressing the secreted form of the West Nile virus envelope glycoprotein protects against West Nile virus encephalitis. J Infect DIS 191:207–214. https://doi.org/10.1086/426824.
29. Higuchi A, Toriniwa H, Komiya T, Nakayama T. 2016. Recombinant measles AIK-C vaccine strain expressing the prM-E antigen of Japanese encephalitis virus. PLoS One 11:e0150213. https://doi.org/10.1371/journal.pone.0150213.
30. Konishi E, Mason PW. 1993. Proper maturation of the Japanese encephalitis virus envelope glycoprotein requires cosynthesis with the premembrane protein. J Virol 67:1672–1675.
31. Schlender J, Schnorr JJ, Spielhoffer P, Cathomen T, Cattaneo R, Billeter MA, ter Meulen V, Schneider-Schaulies S. 1996. Interaction of measles virus glycoproteins with the surface of uninfected peripheral blood lymphocytes induces immunosuppression in vitro. Proc Natl Acad Sci U S A 93:13194–13199. https://doi.org/10.1073/pnas.93.23.13194.
32. del Valle JR, Devaux P, Hodge G, Wegner NJ, McChesney MB, Cattaneo R. 2007. A vectored measles virus induces hepatitis B surface antigen antibodies while protecting macaques against measles virus challenge. J Virol 81:10597–10605. https://doi.org/10.1128/JVI.00923-07.
33. Iankov ID, Haralambieva IH, Galanis E. 2011. Immunogenicity of attenuated measles virus engineered to express *Helicobacter pylori* neutrophil-activating protein. Vaccine 29:1710–1720. https://doi.org/10.1016/j.vaccine.2010.12.020.
34. Hutzler S, Erbar S, Jabulowsky RA, Hanauer JRH, Schnotz JH, Beissert T, Bodmer BS, Eberle R, Boller K, Klamp T, Sahin U, Mühlebach MD. 2017. Antigen-specific oncolytic MV-based tumor vaccines through presentation of selected tumor-associated antigens on infected cells or virus-like particles. Sci Rep 7:16892. https://doi.org/10.1038/s41598-017-16928-8.
35. Laksono BM, Grosserichter-Wagener C, de Vries RD, Langeveld SAG, Brem MD, van Dongen JJM, Katsikis PD, Koopmans MPG, van Zelm MC, de Swart RL. 2018. In vitro measles virus infection of human lymphocyte subsets demonstrates high susceptibility and permissiveness of both naive and memory B cells. J Virol 92. https://doi.org/10.1128/JVI.00131-18.
36. Shan C, Xie X, Shi P-Y. 2018. Zika virus vaccine. Progress and challenges. Cell Host Microbe 24:12–17. https://doi.org/10.1016/j.chom.2018.05.021.
37. Larocca RA, Abbink P, Peron JPS, de A Zanotto PM, Iampietro MJ, Badamchi-Zadeh A, Boyd M, Ng'ang'a D, Kirilova M, Nityanandam R, Mercado NB, Li Z, Moseley ET, Bricault CA, Borducchi EN, Giglio PB, Jetton D, Neubauer G, Nkolola JP, Maxfield LF, De La Barrera RA, Jarman RG, Eckels KH, Michael NL, Thomas SJ, Barouch DH. 2016. Vaccine protection against Zika virus from Brazil. Nature 536:474–478. https://doi.org/10.1038/nature18952.
38. Mrkic B, Pavlovic J, Rülicke T, Volpe P, Buchholz CJ, Hourcade D, Atkinson JP, Aguzzi A, Cattaneo R. 1998. Measles virus spread and pathogenesis in genetically modified mice. J Virol 72:7420–7427.
39. Mura M, Ruffié C, Billon-Denis E, Combredet C, Tournier JN, Tangy F. 2018. hCD46 receptor is not required for measles vaccine Schwarz strain replication in vivo. Type-I IFN is the species barrier in mice. Virology 524:151–159. https://doi.org/10.1016/j.virol.2018.08.014.
40. Engels G, Hierweger AM, Hoffmann J, Thieme R, Thiele S, Bertram S, Dreier C, Resa-Infante P, Jacobsen H, Thiele K, Alawi M, Indenbirken D, Grundhoff A, Siebels S, Fischer N, Stojanovska V, Muzzio D, Jensen F, Karimi K, Mittrücker H-W, Arck PC, Gabriel G. 2017. Pregnancy-related immune adaptation promotes the emergence of highly virulent H1N1 influenza virus strains in allogenically pregnant mice. Cell Host Microbe 21:321–333. https://doi.org/10.1016/j.chom.2017.02.020.
41. Stanelle-Bertram S, Walendy-Gnirß K, Speiseder T, Thiele S, Asante IA, Dreier C, Kouassi NM, Preuß A, Pilnitz-Stolze G, Müller U, Thanisch S, Richter M, Scharrenberg R, Kraus V, Dörk R, Schau L, Herder V, Gerhauser I, Pfankuche VM, Käufer C, Waltl I, Moraes T, Sellau J, Hoenow S, Schmidt-Chanasit J, Jansen S, Schattling B, Ittrich H, Bartsch U, Renné T, Bartenschlager R, Arck P, Cadar D, Friese MA, Vapalahti O, Lotter H, Benites S, Rolling L, Gabriel M, Baumgärtner W, Morellini F, Hölter SM, Amarie O, Fuchs H, Hrabe de Angelis M, Löscher W, Calderon de Anda F, Gabriel G. 2018. Male offspring born to mildly ZIKV-infected mice are at risk of developing neurocognitive disorders in adulthood. Nat Microbiol 3:1161–1174. https://doi.org/10.1038/s41564-018-0236-1.
42. Miner JJ, Cao B, Govero J, Smith AM, Fernandez E, Cabrera OH, Garber C, Noll M, Klein RS, Noguchi KK, Mysorekar IU, Diamond MS. 2016. Zika virus infection during pregnancy in mice causes placental damage and fetal demise. Cell 165:1081–1091. https://doi.org/10.1016/j.cell.2016.05.008.
43. Schaub B, Vouga M, Najioullah F, Gueneret M, Monthieux A, Harte C, Muller F, Jolivet E, Adenet C, Dreux S, Leparc-Goffart I, Cesaire R, Volumenie J-L, Baud D. 2017. Analysis of blood from Zika virus-infected fetuses. A prospective case series. Lancet Infect Dis 17:520–527. https://doi.org/10.1016/S1473-3099(17)30102-0.
44. Baylis SA, Hanschmann K-MO, Schnierle BS, Trösemeier J-H, Blümel J. 2017. Harmonization of nucleic acid testing for Zika virus. Development of the 1st World Health Organization international standard. Transfusion 57:748–761. https://doi.org/10.1111/trf.14026.
45. Combredet C, Labrousse V, Mollet L, Lorin C, Delebecque F, Hurtrel B, McClure H, Feinberg MB, Brahic M, Tangy F. 2003. A molecularly cloned Schwarz strain of measles virus vaccine induces strong immune responses in macaques and transgenic mice. J Virol 77:11546–11554. https://doi.org/10.1128/JVI.77.21.11546-11554.2003.
46. Radecke F, Spielhofer P, Schneider H, Kaelin K, Huber M, Dötsch C, Christiansen G, Billeter MA. 1995. Rescue of measles viruses from cloned DNA. EMBO J 14:5773–5784. https://doi.org/10.1002/j.1460-2075.1995.tb00266.x.
47. Trösemeier J-H, Musso D, Blümel J, Thézé J, Pybus OG, Baylis SA. 2016. Genome sequence of a candidate World Health Organization reference strain of Zika virus for nucleic acid testing. Genome Announc 4. https://doi.org/10.1128/genomeA.00917-16.
48. Kärber G. 1931. Beitrag zur kollektiven Behandlung pharmakologischer Reihenversuche. Arch Exp Pathol Pharmakol 162:480–483. https://doi.org/10.1007/BF01863914.
49. Hubert J. 1984. Spearman-Karber method, p 65–66. *In* Bioassay, 2nd ed. Hunt Publishing, Dubuque, IA.
50. James KT, Cooney B, Agopsowicz K, Trevors MA, Mohamed A, Stoltz D, Hitt M, Shmulevitz M. 2016. Novel high-throughput approach for purification of infectious virions. Sci Rep 6:36826. https://doi.org/10.1038/srep36826.
51. Funke S, Maisner A, Mühlebach MD, Koehl U, Grez M, Cattaneo R, Cichutek K, Buchholz CJ. 2008. Targeted cell entry of lentiviral vectors. Mol Ther 16:1427–1436. https://doi.org/10.1038/mt.2008.128.
52. Malczyk AH, Kupke A, Prüfer S, Scheuplein VA, Hutzler S, Kreuz D, Beissert T, Bauer S, Hubich-Rau S, Tondera C, Eldin HS, Schmidt J, Vergara-Alert J, Süzer Y, Seifried J, Hanschmann K-M, Kalinke U, Herold S, Sahin U, Cichutek K, Waibler Z, Eickmann M, Becker S, Mühlebach MD. 2015. A highly immunogenic and protective Middle East respiratory syndrome coronavirus vaccine based on a recombinant measles virus vaccine platform. J Virol 89:11654–11667. https://doi.org/10.1128/JVI.01815-15.
53. Bodmer BS, Fiedler AH, Hanauer JRH, Prüfer S, Mühlebach MD. 2018. Live-attenuated bivalent measles virus-derived vaccines targeting Middle East respiratory syndrome coronavirus induce robust and multifunctional T cell responses against both viruses in an appropriate mouse model. Virology 521:99–107. https://doi.org/10.1016/j.virol.2018.05.028.
54. Lyons AB, Parish CR. 1994. Determination of lymphocyte division by flow cytometry. J Immunol Methods 171:131–137. https://doi.org/10.1016/0022-1759(94)90236-4.